Journal of Ceramic Processing Research. Vol. 16, No. 2, pp. 244~248 (2015)

J O U R N A L O F
Ceramic Processing Research

Cutting performance and wear mechanism of WC-Co ultrafine cemented carbide during cutting of HT250 gray cast iron

Jian Chen[a], Manfeng Gong[a,b,*] and Shang Hua Wu[a,*]
[a]*School of Electromechanical Engineering, Guangdong University of Technology, Guangzhou, China*
[b]*Institute of Electromechanical Engineering, Lingnan Normal University, Zhanjiang, China*

WC-3TiN-0.8Cr_3C_2-8Co cemented carbides were sintered in de-nitriding and nitriding conditions to use as the cutting tools for HT250 gray cast iron, respectively. Their microstructures and mechanical properties were studied, and the influence of feed rate on tool wear mechanism was investigated. Tool wear mechanism was analyzed by SEM and EDS. Denitriding cemented carbides with the same composition and grain size were prepared for comparison. The results showed that the inserts of nitriding WC-3TiN-0.8Cr_3C_2-8Co cemented carbides possess higher hardness, and better cutting performance than denitriding inserts under the same cutting condition. There were abrasive wear, oxidative wear and obviously abrasive wear on the flank of nitriding inserts. As for denitriding inserts, there were combination of adhesive wear, oxidative wear, built-up-edge (BUE) and abrasive wear on the flank face. Their dominant failure mechanism was abrasive wear. In addition, adhesive wear also played a role in the tools failure to some extent for both nitriding and denitriding cemented carbides cutting tools.

Key words: Cemented carbide, Nitriding, Wear, Failure mechanism.

Introduction

The HT250 gray cast iron, which is brittle, weak and readily machinable, has been used as a wide variety of mechanical components such as cylinder head, cylinder and castings chassis, or other engineering materials. A major reason for the continued large scale uses of cast iron in engineering is not only the desirable properties as good castability and good machinability, but also the economy of machining in terms of cost saving and increase the performance of the product by reducing environmental impact [1-3]. Cemented carbides have been widely used as cutting tool materials for turning of gray cast iron due to their high hardness and outstanding wear resistance [4]. The WC-Co system, which shows an excellent cutting performance for cast iron, is the main type of cemented carbide for a long time. Although the availability of other materials has increased in the cutting tool market, the demands for hard WC-Co material continue to remain strong since it was invented in 1923 [1, 5].

To obtain high wear resistant cemented carbide inserts, there is a promising way to improve their cutting performances by improving hardness during the preparation [6-8]. The hardness, strength, and wear resistance of an alloy increase as the grain size decreases [9, 10]. Many literatures introduced the preparation, microstructure and properties of ultrafine WC-Co cemented carbides [10-14]. At present, ultrafine WC-Co cemented carbides have been widely used for mining, drilling, machining, cutting and forming tools [9]. However, with the increasing demands for higher productivity, improvement of the surface characteristics have been an important subject of many publications and received great attention. Control the nitrogen atmosphere in the sintering chamber during sintering is one of the effective techniques to improve cemented carbides for surface properties [15, 16]. Generally, the refinement of cemented carbides has not been applied to WC-3TiN-0.8Cr_3C_2-8Co cemented carbides, which has more development potential used as cutting tools than the WC-Co cemented carbides [17, 18]. In the present, machining of medium hardened gray cast iron with cemented carbides inserts has become an economical alternative compared to costly CBN and ceramic tool materials. However, machining of harder workpiece puts some restrictions on mechanical properties of cemented carbides inserts and cutting parameters so as to possess the better tool life, dimensional accuracy and surface finish [19]. Therefore, mechanism study on the wear of WC-3TiN-0.8Cr_3C_2-8Co cemented carbide inserts in the hard turning process is extremely valuable and represents a key issue for both tool manufacturers and users.

The first objective of this work was to determine the influence of the nitridation on the wear morphology and wear mechanism of cemented carbides inserts. The second objective of this study was to investigate the influence of feed rate on the wear morphology and wear mechanism of cemented carbides inserts. The cutting

*Corresponding author:
Tel : +0086-020-39322925
Fax: +0086-020-39322925
E-mail: gongmanfeng@163.com, swu@gdut.edu.cn

tests were designed with increasing feed rates, while the depth of cut and cutting speed were kept constant. To the best of the authors' knowledge, few literatures have been reported about WC-3TiN-0.8Cr_3C_2-8Co cemented carbides used as HT250 gray cast iron cutting tool.

Experimental Procedures

Preparation and characterization of WC-3TiN-0.8Cr_3C_2-8Co cemented carbide inserts

The raw material powders used in the present study include WC powder (purity 99.9 wt.%, average oxygen content of 0.05 wt.%, mean particle size of 1 μm), Co (purity 99.9 wt.%, mean particle size of 0.8 μm, TiN (purity 99.9 wt.%, mean particle size of 0.8 μm), Cr_3C_2 (purity 99.9 wt.%, mean particle size of 1 μm), were all commercially bought. Ultrafine WC-3TiN-0.8Cr_3C_2-8Co cemented carbides were prepared according to traditional powder metallurgical procedures. The powders were weighed according to WC-8 wt.% Co-3 wt.% TiN-0.8 wt.% Cr_3C_2, 2 wt.% wax was added as pressing aid and then ball milled in CCl_4 for 48 h with the milling speed of 210 r/min. WC-6 wt.% Co cemented carbides balls with a diameter of 6 mm were used as the milling bodies, the ball to powder weight ratio was selected to be 10 : 1. After milling the pulp was vacuum dried and then sieved through 100 mesh sieves. Two kinds of WC-3TiN-0.8Cr_3C_2-8Co cemented carbides cutting tools marked as AC1604N (nitrided) and AC1604 (denitrided) were pressed for cutting performance test. The pressed pieces (green bodies) were sintered in nitrogen atmosphere (0.1 MPa) of pilot scale according to the thermal cycle as shown in Fig. 1. The comparative inserts sintered in vacuum furnace with the same sintering technology to form the final geometry. The microstructures of the cemented carbides were observed by scanning electron microscope (SEM, NOVA NANOSEM 430), and their phases were characterized by X-ray diffractometer (Bruker D8 Advance). Bulk Vickers hardness measurements of samples were carried out on HV5-30Z Vickers hardness tester, Fracture toughness was determined by means of the palmqvist indentation cracking test by using an indenting load of 10 kg, and density was measured using FA2104J density balance (Satorius, 0.0001 mg sensitive quantity, China) by Archimedes method.

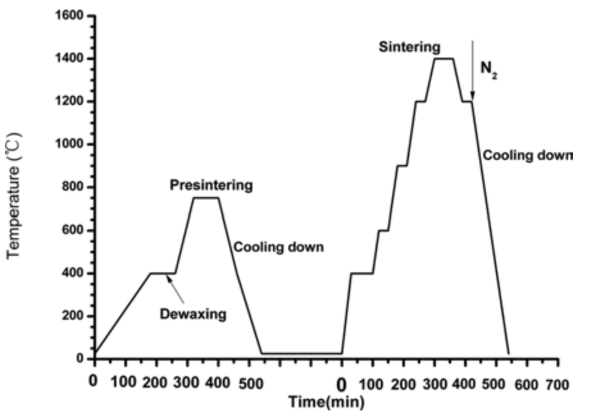

Fig. 1. Thermal cycle of sintering, Nitrogen gas introducing at 1200 ºC.

Cutting tests

All the cemented carbide inserts are grinded for continuous rotating tests. The shape and size of the AC1604N and AC1604 inserts are same as shown in Fig. 2. The experiments are conducted on a CNC lathe with 15 KW of power in the spindle motor under dry cutting condition. Two kinds of WC-3TiN-0.8Cr_3C_2-8Co cemented carbides cutting tools, AC1604N (nitrided) and AC1604 (denitrided), are clamped in a left-hand tool holder (CSSNL2525M1207) with 45 º lead angle and 8 º30' rake angle. The workpiece is HT250 gray cast iron bar with 100 mm diameter and 150 mm length. The chemical composition and mechanical properties of the workpiece are listed in Table 1.

The cutting parameters for tests are listed in Table 2. The total cutting time was fixed at 20 min for all the cutting parameter combinations since the objective of the paper was not to carry out tool life research but to investigate the wear evolution and mechanism. Coolant was not used during cutting, and a fresh cutting edge was used for each test. After each test, flank worn surface of the cemented carbide insert was ultrasonically cleaned with acetone. Then the flank wear (VB) and tool breakage were investigated by an optical tool microscope. The worn surfaces of cemented carbides inserts at the

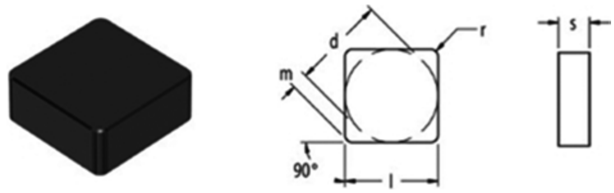

Fig. 2. Schematic of the AC1604N (AC1604) cemented carbide type insert, $l = d = 12.76(\pm 0.025$ mm), $s = 4.76(\pm 0.025$ mm), $r = 0.8$ mm.

Table 1. Chemical composition and mechanical properties of gray cast iron.

Chemical composition of gray cast iron (wt.%)				
C	Si	Mn	S	P
3.16-3.30	1.79-1.93	0.89-1.04	0.094-0.125	0.120-0.170
Mechanical properties				
Hardness (RH = 1) 209 HB Tensile strength 250 MPa				

Table 2. Testing details for cutting performance.

Experiment number	f (mm/r)	a_p (mm)	Vc (m/min)
1	0.2	0.1	120
2	0.4	0.1	120
3	0.6	0.1	120

end of cut were observed under a scanning electronic microscope (SEM) coupled to an energy dispersive spectroscopy (EDS) system to examine the nature of the worn rake and flank face to understand the wear mechanism.

Results and Discussion

Microstructures and properties of both inserts

The SEM images of AC1604 and AC1604N cemented carbides inserts used in the study were shown in Fig. 3. Samples sintered in vacuum furnace show incomplete sintering with rounded WC grains and cobalt "lakes" along with micropore. However, WC grains of AC1604N cemented carbides inserts appear with prismatic angles and the cobalt distribution got more uniform with full density. The majority of grains belong to the normal growth but a few abnormal growth grains exist. The reason is that cobalt conglomerations become a "cobalt pool", and in this area the WC grains are directly contacted with each other, which results in the abnormal grain growth. Fig. 4 showed WC grain size distribution in the two cases of AC1604N and AC1604. Both show reasonably continuous distribution, but AC1604N shows a narrower distribution with little absence of grains over 1.2 μm. It can be seen that the WC of AC1604N cemented carbides have a mean grain size of approximate 0.45 μm. However, the AC1604 cemented carbides show an average WC grain size of 0.85 to 0.95 μm. The different microstructures largely influence on the mechanical properties and the cutting performances for both cemented carbide inserts.

Low magnification microstructures and mechanical properties of both inserts are listed in Table 3. According to the ISO norm 4505 (Hardmetals Metallographic determination of porosity and uncombined carbon), pores up to 10 μm are designated as "A" pores and those larger than 10 μm but smaller than 25 μm are called "B" pores [20]. Both polished inserts show only type "A" porosity with a concentration of A02, hence, WC-3TiN-0.8Cr_3C_2-8Co inserts with full density were achieved. Both inserts show similar density due to the same nominal chemical composition and sintering temperature. The hardness of alloys and compounds is determined by the grain size deduced from the Hall-Petch relationship

Table 3. Low magnification microstructure and mechanical properties of both cemented carbides.

Inserts	AC1604N	AC1604
Low magnification microstructures	A02B00C00	A02B00C00
Density (g/cm^3)	13.15	13.04
Hardness (HV_{10})	2140 ± 35	1780 ± 28
Fracture toughness ($MPa \cdot m^{1/2}$)	4.2	3.1

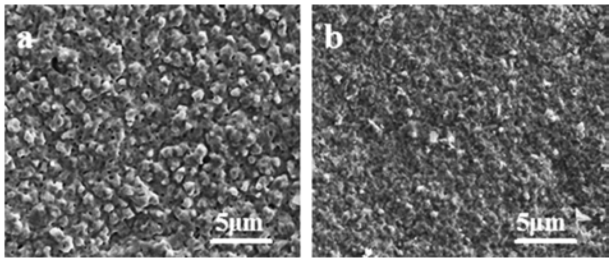

Fig. 3. SEM images of both cemented carbide inserts. (a) AC1604, (b) AC1604N.

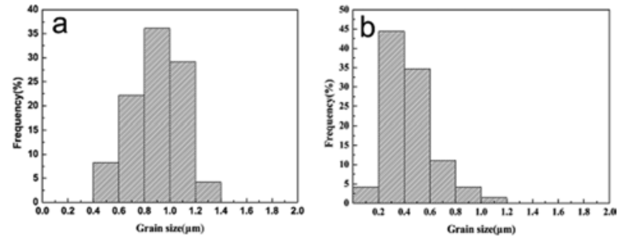

Fig. 4. Grain size distribution, (a) AC1604, (b) AC1604N.

[12]. If the grain size of WC is small, more and more WC grains dissolve in the Co binder phase and the hard phase distributes uniformly in all cemented carbides matrixes which increase the bonding strength of hard phase [6]. The AC1604N cemented carbides show larger hardness of 2150 HV_{10}. Generally, AC1604N cemented carbides possess better mechanical properties than Vacuum sintered inserts with the same composition.

Wear mechanism

Flank wear morphology and wear mechanism of both AC1604N and AC1604 cemented carbides inserts after machining with different feed rates are discussed with the images taken by SEM. The EDS analysis of the flank wear surfaces are shown in Fig. 6. The contact friction between tool and workpiece generated high temperatures on the cutting tool. Therefore the main type of tool wear gradually occurred on the top flank face [23].

The flank wear morphologies of AC1604N and AC1604 cemented carbides inserts after the turning tests are shown in Fig. 5. The flank wear morphologies between AC1604N and AC1604 inserts are largely different. In the case of AC1604N insert, the wear behavior was typical abrasive wear, which is the removal of grains from tool material by the work material, and subsequently produces a rough area. In addition, small adhered particles were found on worn surface, which were come from the workpiece during the turning tests. There was no serious flank wear when the cutting test was finished with a feed rate of 0.2 mm/r (see Fig. 5(a)). With the feed rate increased to 0.4 mm/r, there was slight wear on the flank face with a VB value of 0.14 mm. Many adhered particles were observed on worn surface. When the feed rate increased to 0.6 mm/r, there existed obvious flank wear of 0.22 mm. The combination of abrasive wear and adhesive wear were observed. A great deal of

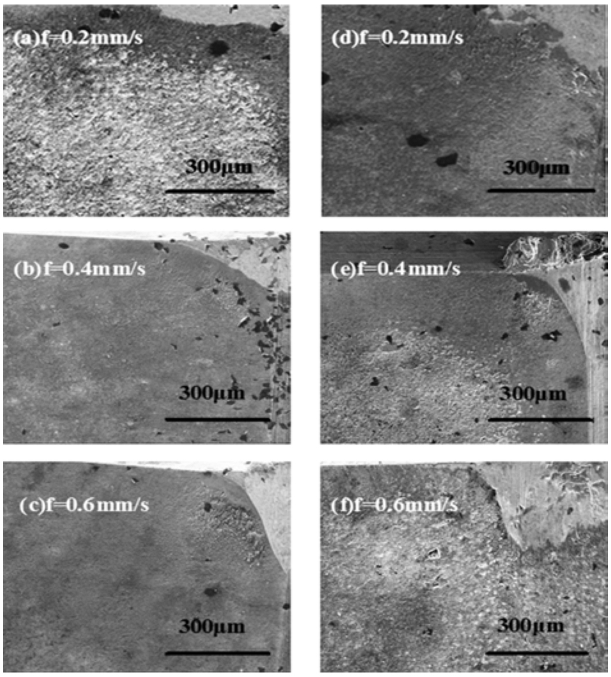

Fig. 5. the flank wear morphology of both AC1604N (a, b, c) and AC1604 (d, e, f) cemented carbide inserts machined with different feed rates shown in the top left of each figure.

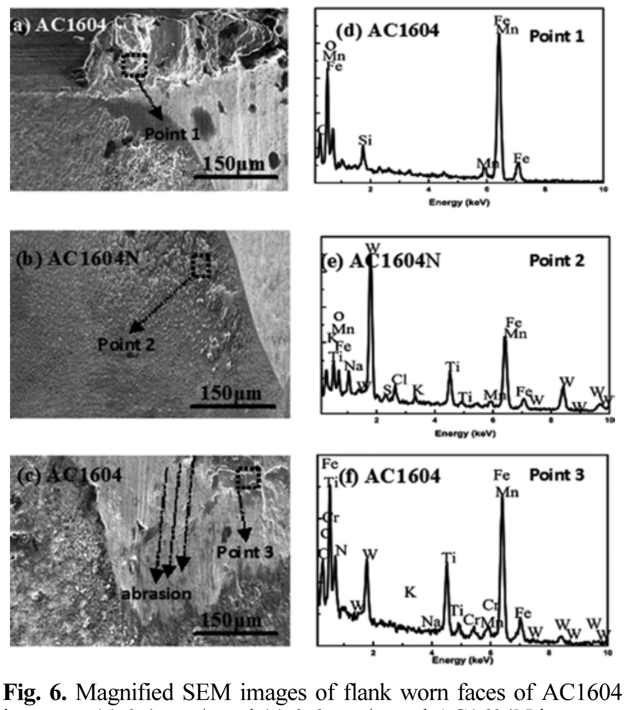

Fig. 6. Magnified SEM images of flank worn faces of AC1604 inserts at (a) 0.4 mm/s and (c) 0.6 mm/s; and AC1604N inserts at (b) 0.4 mm/s for 30 min cast iron turning. EDS patterns of Point 1 in (d), Point 2 in (e) and Point 3 in (f), respectively.

workpiece material adhered on the flank surface of the tool, as is shown in Fig. 5(c) or Fig. 6(b). The weak Fe peaks (see Fig. 6(b)) indicate the existence of slight adhesion wear on the worn flank face. Furthermore, O element (see Fig. 6(b)) can be detected by the EDS analysis of the flank surfaces for the AC1604 inserts after turning tests. This is an indication of the formation of softer oxide such as Co_3O_4, CoO, WO_3 and TiO_2, which inevitably cause oxidative wear.

In the case of AC1604 inserts, flank wear with a VB value of about 0.04 mm appeared when the cutting test was finished with a feed rate of 0.2 mm/r. When the feed rate increased to 0.4 mm/r, the flank wear VB value was 0.09 mm. As the turning process continues, the friction area is widened, which causes the increase of cutting temperature, leading to the formation of built-up-edge (BUE) on the flank face, as shown in Fig. 5(e) or Fig. 6(a). The formation of the BUE can be mainly due to the strong interaction of the AC1604 inserts with the gray cast iron at high cutting contact temperatures. It was confirmed by the elemental analysis that remarkable high adhesion of Fe and Mn were observed from the BUE of the flank face, as shown in Fig. 6(d). These adhered layers of cast iron accelerate wear mechanisms such as attrition, abrasion and/or diffusion [24]. When the feed rate increased to 0.6 mm/r, the friction and pressing effect of the workpiece on the cutting edge was more serious and the flank wear increased fast to 0.27 mm. This indicates that AC1604N insert is harder than AC1604 insert to meet the wear resistance. Furthermore, the smooth surface of AC1604N insert can potentially decrease the friction between the cutting insert and workpiece. The decreased fiction is beneficial to the chip evacuation and reducing the wear rate. There were many grooves and workpiece material adhered on the flank of the AC1604 inserts as shown in Fig. 5(f) or Fig. 6(c). The presence of Fe and Mn peaks from EDS analysis (see Fig. 6(f)) confirmed the adhesive wear owing to tool wear. Meanwhile, O element can be detected by the EDS analysis (see Fig. 6(f)), which was the evidence of oxidative wear.

Generally, tool flank wear formed due to the friction between the machined surfaces and the flank face of the inserts. During the cutting process, abrasive wear occurred when hard workpiece material chippings or escaped hard tool particles of tool materials moved across the contact area. Therefore, abrasive wear was the predominant flank wear mechanism of both inserts. Since AC1604N cemented carbide inserts have well dispersed ultrafine WC and TiN hard phases, the inserts showed higher hardness and better wear resistance during cutting. Therefore, the AC1604N insert showed less serious flank wear compared to the AC1604 insert.

Conclusions

The following conclusions can be drawn from this investigation on turning of HT250 gray cast iron using both AC1604N and AC1604 cemented carbides inserts at different feed rate:

(1) The AC1604N inserts showed higher hardness and fracture toughness of 2140 ± 35 HV_{10} and 4.2 $MPa \cdot m^{1/2}$, compared to 1680 ± 28 HV_{10} and 3.1 $MPa \cdot m^{1/2}$ of AC

1604 inserts.

(2) The combination of abrasive wear, oxidative wear and adhesive wear were observed on the flank wear of AC1604N inserts. The combination of adhesive wear, oxidative wear, built-up-edge (BUE) and abrasive wear were observed on the flank wear of AC1604 inserts. The dominant failure mechanism on the flank face of AC1604 inserts were abrasive wear and adhesive wear.

(3) For HT250 gray cast iron turning, a built-up-edge (BUE) was formed on the flank face which can be mainly due to the strong interaction of cemented carbides inserts with the workpiece material at high cutting contact temperatures.

(4) There was a transition from abrasion predominant wear mechanism to adhesive wear on the flank face of AC1604N inserts with the increase of feed rate. In the case of AC1604 inserts, there existed amazing adhesive wear and abrasive wear, and built-up-edge usually formed on the flank face.

Acknowledgments

The present work was financially supported by the Project supported by Research Founding for Introduction of Leading Talents of Guangdong Province (400120001), Research Funding for Introduction of Guangdong Province Leading Talents (Grant No. 40012001), Natural Science Foundation of Guangdong Province (S2013010013385) and Program for Innovative Research Team in Zhanjiang Normal University (ZSIRT13006).

References

1. J.V.C. Souza, M.C.A. Nono, M.V. Ribeiro, J. P. B. Machado, and O.M.M. Silva, Mater.Des. 30 [7] (2009) 2715-2720.
2. A.A. Pereira, L. Boehs, and W.L. Guesser, J. Mater. Process. Technol. 179 [1] (2006)165-171.
3. K. DeBenedictis, Manuf. Eng. 119 [3] (1997) 48-50.
4. A. Upadhyaya, D. Sarathy, and G. Wagner, Mater. Des. 22 [6] (2001) 499-506.
5. O. Seo, S.Kang, and E.J. Lavernia, Mater. Trans. 44 [11] (2003) 2339-2345.
6. Y. Wang, Z,-y. Pan, C,-b. Wang, X,-g. Sun, Z,-j. Peng, and B,-l. Wang. J. Mater. Sci. Technol. 28 [3] (2012) 205-213.
7. L. Espinosa, V. Bonache, M.D. Salvador. Wear, 272 [1] (2011) 62-68.
8. R. van der Merwe, N. Sacks. Int. J. Refract. Met. Hard Mater. 41 (2013) 94-102.
9. D,-h. Xiao, Y,-h. He, M. Song, N. Lin, and R,-f. Zhang. Int. J. Refract. Met. Hard Mater. 28 [3] (2010) 407-411.
10. D,-h. Xiao, Y,-h. He, W,-h. W,-h. Luo, and M. Song. Trans. Nonferrous Met. Soc. China. 19 [6] (2009) 1520-1525.
11. T,-t. Shen, D,-h. Xiao, X,-q. Ou, M. Song, Y,-h. He, N. Lin, and D,-f. Zhang. J. Alloys Compd. 509 [4] (2011) 1236-1243.
12. L. Sun, C,-c. Jia, R,-j. Cao, and C,-g. L. Int. J. Refract. Met. Hard Mater. 26 [4] (2008) 357-361.
13. H,-y. Rong, Z,-j. Peng, X,-y. Ren, C,-b. Wang, L,-h. Qi, and H,-z. Miao. Int. J. Refract. Met. Hard Mater. 29 [6] (2011) 733-738.
14. X,-y. Ren, Z,-j. Peng, Y. Peng, C,-b. Wang, Z,-q. Fu, L,-h. Qi, and H,-z. Miao. Int. J. Refract. Met. Hard Mater. 41 (2013) 308-314.
15. J.R. Conrad, J.L. Radtke, R.A. Dodd, F.J. Worzala, and N.C. Tran, J. Appl. Phys. 62 [11] (1987) 4591-4596.
16. J. Garcia, R. Pitonak, Int. J. Refract. Met. Hard Mater. 36 (2013) 52-59.
17. D. Duman, H. Gökçe, and H. Çimenoğlu. J. EUR. CERAM. SOC. 32 [7] (2012) 1427-1433.
18. K.H. Lee, S.I. Cha, B.K. Kim, and S.H. Hong. Int. J. Refract. Met. Hard Mater. 24 [1] (2006) 109-114.
19. S. Chinchanikar, S.K. Choudhury. Meas. 46 [4] (2013) 1572-1584.
20. S.K. Bhaumik, G.S. Upadhyaya, and M.L. Vaidya. J. Mater. Process. Technol. 58 [1] (1996) 45-52.
21. W,-h. Tarng, Y,-s Yang. J.Mater.Process.Technol. 84 [1] (1998) 122-129.
22. X. Luo, K. Cheng, R. Holt, and X. Liu. Wear, 259 [7] (2005) 1235-1240.
23. T. Sugihara, T. Enomoto, Precis. Eng. 37 [4] (2013) 888-896.
24. H. Çalşþkan, C. Kurbanoğlu, P. Panjan, M. Cekada, and D. Kramar. Tribol. Int. 62 (2013) 215-222.